IEEE Access
Multidisciplinary | Rapid Review | Open Access Journal

Received August 18, 2019, accepted August 25, 2019, date of publication August 27, 2019, date of current version September 9, 2019.

*Digital Object Identifier 10.1109/ACCESS.2019.2937888*

# Bidirectional Undersea Capacitive Wireless Power Transfer System

**LEI YANG, (Member, IEEE), MINNA JU, AND BEN ZHANG**
Shaanxi Key Laboratory of Complex System Control and Intelligent Information Processing, School of Automation and Information Engineering, Xi'an University of Technology, Xi'an 710048, China

Corresponding author: Lei Yang (yanglei0930@gmail.com)

This work was supported in part by the China Postdoctoral Science Foundation under Grant 2018M643700, in part by the Scientific Research Project of Education Department of Shaanxi Province under Grant 18JS080, and in part by the Postdoctoral Research Grant Project of Shaanxi Province, China.

**ABSTRACT** This paper proposes a bidirectional undersea capacitive wireless power transfer system (BD-UCWPT) for the autonomous underwater vehicles (AUVs). The two H-Bridge circuits are adapted in the proposed BD-UCWPT system to achieve the bidirectional power flow. The H-Bridge circuit is built based on the GaN devices. As a result, the high switching frequency, and low power loss could be reached. The two LCLC compensation networks are respectively used in the transmitter side and receiver side. The simulation work is conducted with the Ansys Maxwell, PSIM and MATLAB. In the experiments, two seawater bags are added in the middle of two metal plates of $C_{S1}$ and $C_{S2}$ to model the seawater condition, respectively. In order to verify the theory analysis, a 100W experimental BD-UCWPT system is constructed. The experiments have been conducted in air and in seawater, respectively. The simulated and experimental results are compared with each other. It shows that, with this BD-UCWPT system, the power of AUVs could flow bidirectionally. The stable operation and high efficiency of BD-UCWPT system is verified. The research work in this paper could facilitate the application of wireless power transfer (WPT) system for AUVs and other undersea devices.

**INDEX TERMS** Wireless power transfer system, bidirectional, undersea, autonomous underwater vehicles (AUVs).

## I. INTRODUCTION

Wireless power transfer (WPT) system has attracted more and more attentions in recent years, which is developed to deliver power to electrical equipment in different areas, contactlessly. There are two different types of WPT systems: one is capacitive wireless power transfer (CWPT) system [1]–[3], the other is the inductive wireless power transfer (IPT) system [4]–[7]. IPT system transfers the power wirelessly by adapting magnetic field with the inductive coils. However, the power is transferred by the CWPT system through the high frequency alternating electric fields. With the IPT system, the power could be transferred with the high efficiency and high capacity. It has been widely used for mobile phones [8], [9], biomedical devices [10], [11], sensor networks [12], [13], electrical vehicles [14]–[16] and autonomous underwater vehicles (AUVs) [17]. The DC-DC efficiency could be over 90% with the resonant network and the transfer distance could be reached several hundreds of mm. The IPT system has been used in the undersea condition with the good performance. The new design with the two decoupled receivers composed of two reversely wound receiver coils. This system could deliver the power level more than 600W with a maximum DC-DC efficiency 92.6% as shown in [18]. Paper [19] provides a three-phase wireless charging system for lightweight AUVs. The power transfer efficiency is 92.41% at frequency 465kHz. Its power level is 1.0kW [19].

In order to have a good analysis of underwater or undersea wireless power transfer (UWPT) system, the eddy current loss in seawater is deeply studied in different circumstances in [20]. It shows that the optimum resonant frequency will be shifted because of the eddy current loss in seawater. Paper [21] proposes a maximum power efficiency tracking (MPET) method to estimate the system's coupling coefficient and to track the peak efficiency. A structure of 4-layered spiral coil resonators is provided in [22] for UWPT system. The efficiency is improved with this new structure.

However, as shown in [23], the IPT system is very sensitive to conductive objects such as metal debris around it. On the other hand, the magnetic fields will generate the eddy current

The associate editor coordinating the review of this article and approving it for publication was Zhixiang Zou.

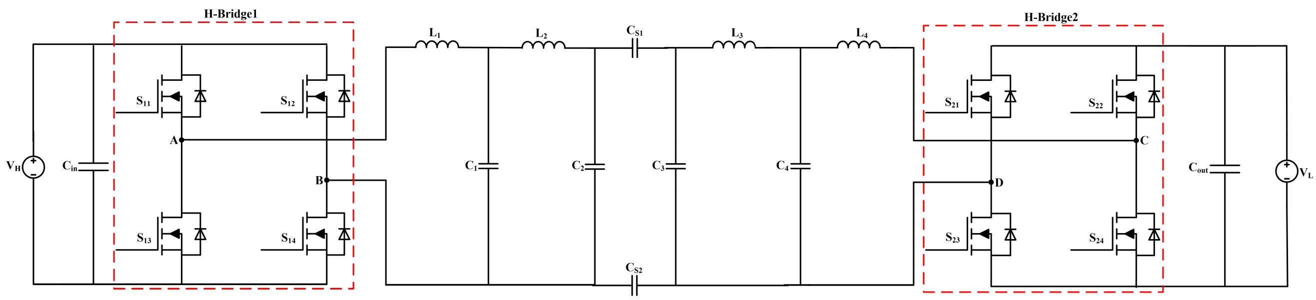


**FIGURE 1.** Topology of BD-UCWPT system.

losses in the metals which is located near the IPT system. The temperature will be highly increased which is dangerous to the human beings or animals in practice. In order to solve the above-mentioned problems of IPT system, the CWPT system is a good answer.

The CWPT system could use the electric fields to transfer power to replace the magnetic fields. With the electric fields, the significant power losses could be removed [24]. As the allium metal plates are adapted, the price of WPT system could be rapidly cut down. It is easier to design a capacitive metal plates than the inductive coils. In recent years, CWPT system has been deeply studied. A double-sided LCLC compensated CWPT system is proposed in [23], which is developed for the electrical vehicle. The 2.4kW power level is designed with the four copper plates (size 610mm×610mm). The maximum efficiency of proposed CWPT system is 90.8%. Paper [24] presents a four-plate compact capacitive coupler CWPT system with the LCL compensated topology. To save space, the four plates are placed vertically instead of horizontally. The 85.87% efficiency was achieved with 1.88kW output power at the 150mm air-gap distance. An inductive and capacitive combined parallel transmission of power and data WPT system is shown in [25]. The inductive channel is used to transfer the energy and the capacitive channel is adapted to transfer data. Paper [26] develops wireless battery charging system for an unmanned aerial vehicle or drones based on the CWPT system. It operates at frequency 6.78MHz and its power level is 12W. The tested efficiency is about 50%. Paper [27] presents a novel one-kilowatt CWPT system via wheels of a compact electric vehicle. In this paper, a high KQ capacitive coupling scheme is built. The tested efficiency is about 80%. A power maximization for CWPT system is presented in [28]. It adapts two transmitters and one receiver. Paper [29] proposes a CWPT system for LED driver. The isolation function is verified by simulation and experiments. A Z-impedance compensation for CWPT system is developed in [30]. With a 5W topology, the proposed compensation network exhibit the open-circuit and short circuit immunity, it could boost up the output voltage by 50%.The power loss characteristics of CWPT system is shown in [31].The power loss is analyzed under the condition of output power 200W with the LC resonant circuit. Its operation frequency is 1MHz. Paper [32] introduces a CL compensation circuit on the secondary side to reduce the voltage stress across the electric field coupling interface. It shows that the quality factor could be reduced to make the system less sensitive to circuit parameter and load variations by increasing capacitance. A high power-density CWPT system is presented in [33].The resonant frequency is set 6.78MHz by adapting GaN-based devices. With the zero-voltage switching, the 90.4% efficiency is achieved. The power density of proposed CWPT system is 51.4kW/m2. In [34], a DC-DC converter is used to track the maximum output power of a CWPT system. A perturb and observe algorithm is developed for controlling the duty-cycle of the DC-DC converter to track the maximum power against load variations. The 70% efficiency is achieved with a wide range load variation from 5Ω to 500Ω.

When it comes to the UWPT system, there is very few research papers. A CWPT system is proposed in [35] for operation. This CWPT system is used for the AUVs. It achieves the 91.3% efficiency at the power transfer distance of 20mm. Howevr, the proposed CWPT system is just used for the fresh water. The power could be transferred in one way-from the power station to the AUVs.

To authors' best knowledge, there is no CWPT system which is used in undersea condition. With the good performance of CWPT system, the research on the undersea capacitive wireless power transfer (UCWPT) system will facilitate the applications of WPT system for smart ocean energy system. In the future, the AUVs will provide more good performance if the power could be flowed bidirectionally. It means that one AUV could be charged by the WPT station and discharge its stored energy to other AUV. In order to achieve this function, the bidirectional undersea capacitive wireless power transfer (BD-UCWPT) system should be studied and analyzed.

This paper proposes a novel BD-UCWPT for AUVs and other undersea equipment. The rest of paper is organized as follows: Section II provides the theory analysis. The simulated and experimental verification is shown in Section III. The conclusions and discussions are drawn in Section IV.

## II. THEORY ANALYSIS

As shown in Fig. 1, the proposed BD-UCWPT system will be used for AUVs. An AUV will be charged by the undersea charging station and discharge its energy to other AUV through the electric fields. It can be seen from Fig. 2, the DC

 

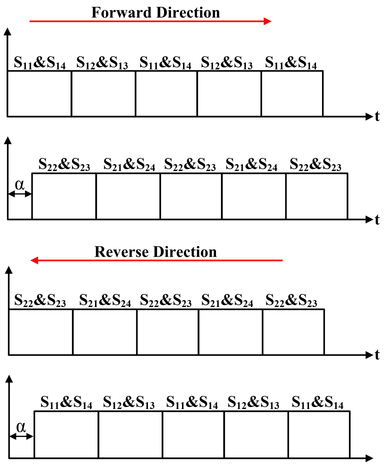


**FIGURE 2.** PWM waveforms of BD-UCWPT system.

power source will be firstly inverted to AC voltage for the transmitter by the H-bridge 1. Then, the power will be wirelessly transferred from the transmitter to the receiver through the capacitive channels. The H-bridge 2 at the receiver side will act as a rectifier to change the AC voltage to the DC voltage for the load.

The equivalent operation states are shown as Fig. 3, the power flows from the $V_H$ to $V_L$. In this paper, the forward power flow is taken as an example (from the $V_H$ to $V_L$).

In the transmitter side, it can be seen from Fig. 3(a), when switches $S_{11}$ and $S_{14}$ are turned on and $S_{12}$ and $S_{13}$ are turned off, the current of the power source flows through the transmitter in the forward direction. The LCLC compensation network at the transmitter side will work at the resonant frequency. In the receiver side, as shown in Fig. 3(a), when switches $S_{22}$ and $S_{23}$ are ON while switches $S_{21}$ and $S_{24}$ are OFF, the positive half cycle of the alternating current of receiver will charge the filter capacitor and the $V_L$. At the same time, the LCLC compensation network at the receiver side will work at the resonant frequency. The filter capacitor will transfer its energy to the $V_L$. The power is wirelessly transferred.

As shown in Fig. 3(b), when switches $S_{12}$ and $S_{13}$ are turned on and $S_{11}$ and $S_{14}$ are turned off, the current of the power source will flow through the transmitter in the reverse direction. During this time period, the LCLC compensation network on the transmitter side will work at the resonant frequency. It can be seen from Fig. 3(b), when switches $S_{21}$ and $S_{24}$ are ON while switches $S_{22}$ and $S_{23}$ are OFF, the negative half cycle of the alternating current of receiver will flow through the filter capacitor and the $V_L$. During this time period, the LCLC compensation network on the receiver side will work at the resonant frequency. At the same time, the filter capacitor will transfer its energy to the $V_L$. As a result, the power is wirelessly transferred with the proposed BD-UCWPT system.

The power which is transferred from the receiver to the transmitter is similar to the operation of the forward direction power operation of proposed BD-UCWPT. In one switching cycle, in the forward direction, the power is transferred from $V_H$ to $V_L$. In the reverse direction, the power is transferred from $V_L$ to $V_H$.

As shown in Fig. 1, the equivalent capacitance could be written as:

$$C_s = C_{s1} \times C_{s2} / (C_{s1} + C_{s2}) \tag{1}$$

Considering the edge effects, one single capacitor, with the seawater medium, can be calculated:

$$C_{s1} = C_{s2} = [1 + 2.343 \times (\frac{d}{l})^{0.891}] \times (\varepsilon_{sea} \times \frac{(l)^2}{d}) \tag{2}$$

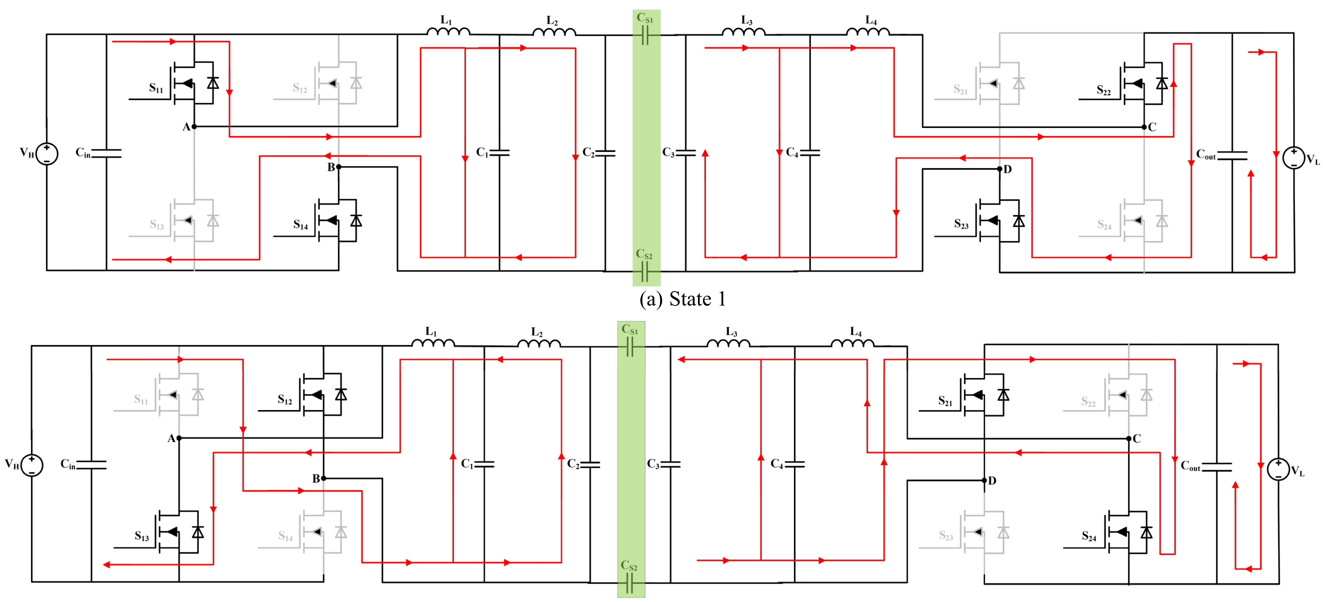

(a) State 1

(b) State 2

**FIGURE 3.** Operation states of proposed BD-UCWPT system.

where 1 is the length of metal plate, d is the distance of one pair of plates, and $\varepsilon_{sea}$ is the permittivity of seawater.

As shown in [36], the permittivity of seawater, temperature, salinity and angular frequency of electromagnetic wave have a relationship as:

$$\varepsilon(S,T,\omega)=\varepsilon_{\infty}(S,T)+\frac{\varepsilon_1(S,T)-\varepsilon_{\infty}(S,T)}{1-j\omega\tau(S,T)}-j\frac{\delta(S,T)}{\omega\varepsilon_0} \quad (3)$$

where $\varepsilon_{\infty}(S,T)$ is the seawater dielectric permittivity high-frequency limit, dimensionless (the value is 4.9); $\varepsilon_0 = 8.854\times10^{-12}Fm^{-1}$ is the permittivity of free space; $\omega = 2\pi f$, f is the frequency of electromagnetic wave;$\varepsilon_1(S,T)$ is the static permittivity of seawater and $\delta(S,T)$ is the ionic conductivity of seawater.

The static permittivity of seawater and the ionic conductivity of seawater are respectively written as (4) and (5), as shown at the bottom of the next page.

The relaxation time of seawater could be derived as (6), as shown at the bottom of the next page.

Setting the voltage of capacitor $C_1$ is equal to $V_1$, the voltage of capacitor $C_2$ could be written as:

$$V_{C2}=-\frac{C_1}{C_T}V_1 \quad (7)$$

Based on Fig. 1, the voltage of $C_4$ could be derived as

$$V_{C4}=V_{C3}\times\frac{-C_s\times C_1}{C_2C_s+C_3C_s+C_2C_3}\times V_1 \quad (8)$$

where $V_1$ is the voltage between points A and B of H-Bridge 1.

The current of inductor $L_1$ could be written as:

$$I_1=V_1\times\frac{C_1}{C_T}\times\frac{C_s}{C_s+C_3}\times\frac{1}{j\omega L_4} \quad (9)$$

The output power could be derived as:

$$P_{out}=\omega C_s\times\frac{C_1C_4}{C_2C_3+C_2C_s+C_3C_s}\times|V_1|\times|V_2| \quad (10)$$

where $V_2$ is the voltage between points C and D of H-Bridge 2.

In the resonant condition, the rms voltage of capacitor $C_4$ is equal to the rms voltage of inductor $L_4$. It can be presented as:

$$U_{C4}=U_{L4} \quad (11)$$

The current of capacitor $C_4$ is derived as:

$$I_{C_4}=U_{C_4}\times j\omega C_4 \quad (12)$$

The voltage of capacitor $C_2$ could be written as:

$$U_{C2}=j\omega L_2I_1 \quad (13)$$

According to Fig. 1, the $V_{AB(t)}$ of H-Bridge 1 could be written as:

$$V_{AB(t)}=\frac{4}{\pi}V_{in}\sin(2\pi f_s t) \quad (14)$$

Then, the rms value if $V_{AB(t)}$ could be derived as:

$$V_{AB}=\frac{2\sqrt{2}}{\pi}V_{in} \quad (15)$$


**FIGURE 4.** BD-UCWPT experimental prototype.

As shown in Fig. 1, the the $V_{CD(t)}$ of H-Bridge 2 could be written as:

$$V_{CD(t)}=\frac{4}{\pi}V_{in}\sin(2\pi f_s t-\varphi) \quad (16)$$

Then, the rms value of $V_{CD(t)}$ could be derived as:

$$V_{CD}=\frac{2\sqrt{2}}{\pi}V_o \quad (17)$$

## III. SIMULATION AND EXPERIMENTAL VERFICATION

In order to illustrate the viability of the proposed BD-UCWPT system and to verify the accuracy of the theory analysis, a 100W 'proof of concept' prototype shown in Fig. 4. It can be seen from Fig. 4, the experimental prototype is composed by the two H-Bridges (H-Bridge 1 and H-Bridge 2), two LCLC compensation networks, load resistor and filter capacitor. The resonant frequency is set 625kHz. As shown in Fig. 4, in the experiments, two seawater bags are respectively placed in $C_{S1}$ and $C_{S2}$ to model the seawater medium. The circuit parameters of proposed BD-UCWPT system is shown as Table 1. The simulation is conducted with Ansys Maxwell, PSIM and MATLAB. The input voltage and input current are tested to calculate the input power. What's more, the load voltage and load current are tested to calculate the load power. The experiments are conducted under different distances between transmitter and receiver (3cm, 5cm, 8cm, 10cm, and 15cm). What's more, the experiments are conducted in air and seawater to test the performance of proposed BD-UCWPT system. The proposed BD-UCWPT system is controlled by the open-loop synchronous control method or phase-shift control method. In the forward direction power flow, the $V_H$ acts as the power source while the $V_L$ is replaced by the load resister. In the reverse direction, the $V_L$ acts as the power source while the $V_H$ is replaced by the load resister.

### A. SIMULATED VERRIFICATION

The simulation is conducted with the load resistance 100Ω. The BD-UCWPT system is controlled with the open-loop

**TABLE 1. Comparison with prior art.**

| UWPT | Power Level | Efficiency | Frequency | Transfer Distance | Bidirectional or Not | Seawater or Freshwater | Power Transfer Medium |
|---|---|---|---|---|---|---|---|
| Paper [19] | 1kW | 92.4% | 465kHz | 21mm | Not | Seawater | Magnetic Fields |
| Paper [21] | 40W | 80% | 178kHz8 | 100mm | Not | Seawater | Magnetic Fields |
| Paper [35] | 400W | 90% | 107.7MHz | 20mm | Not | Freshwater | Electronic Fields |
| Paper [37] | Undescribed | 88% | 100kHz | 150mm | Not | Seawater | Magnetic Fields |
| Paper [38] | Undescribed | 80% | 20kHz | 75mm | Not | Seawater | Magnetic Fields |
| Paper [39] | Undescribed | 80% | 110kHz | 20mm | Not | Seawater | Magnetic Fields |
| Paper [40] | 75W | 85% | 300KHz | 50mm | Not | Seawater | Magnetic Fields |
| This Work | 100W | 80.15% | 625KHz | 150mm | Bidirectional | Seawater | Electronic Fields |

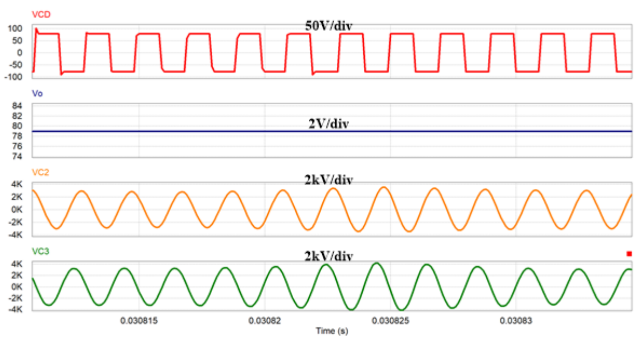


**FIGURE 5. Operation waveforms of BD-UCWPT system with the load resistance 100Ω in the forward direction.**

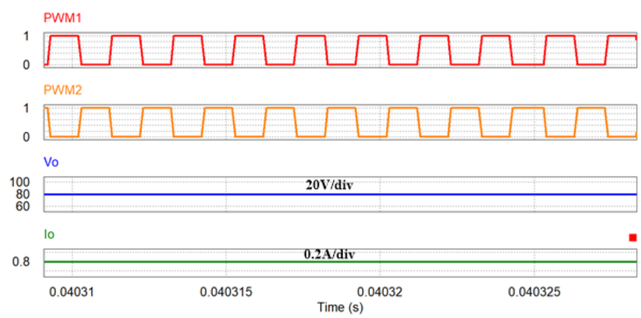


**FIGURE 6. Simulated load voltage and load current of BD-UCWPT system with the load resistance 100Ω in the forward direction.**

synchronous control method. When the power is transferred from $V_H$ to $V_L$, the H-Bridge1 is used as an inverter and H- Bridge 2 is adapted as a rectifier. The input voltage varies from 0-100V and the frequency is 625kHz. When the power is transferred from $V_L$ to $V_H$. The H-Bridge 2 is acted as an inverter and H-Bridge 1 is used as a rectifier. The input voltage changes from 0-100V and the resonant frequency is set 625 kHz. The simulated results are presented in Fig. 5 and Fig. 6. As shown in Fig.5 and Fig.6, the proposed BD-UCWPT system works in the resonant condition.

It can be seen from Fig. 5 and Fig. 6, with the open-loop synchronous control method, the load voltage is about 80V at the load resistance 100Ω in the forward direction. The proposed BD-UCWPT system works in the resonant condition and the power is transferred through the electric fields.

$$\varepsilon_1(S,T) = (87.134 - 0.1949T - 0.01276T^2 + 0.0002491T^3) \times (1 + 1.613\times10^{-5}TS - 0.003656S + 3.21\times10^{-5}S^2 - 4.232\times10^{-7}S^3) \quad (4)$$

$$\sigma(S,T) = S(0.182521 - 0.00146192S + 2.09324\times10^{-5}S^2 - 1.28205\times10^{-7}S^3) \times \exp((T-25)(0.0203 + 0.0001266(25-T) + 2.464\times10^{-6}(25-T)^2 - S(1.849\times10^{-5} - 2.551\times10^{-7}(25-T) + 2.551\times10^{-8}(25-T)^2))) \quad (5)$$

$$\tau(S,T) = (1.768\times10^{-11} - 6.086\times10^{-13}T + 1.104\times10^{-14}T^2 - 8.111\times10^{-17}T^3) \times (1.0 + 2.282\times10^{-5}TS - 7.638\times10^{-4}S - 7.760\times10^{-6}S^2 + 1.105\times10^{-8}S^3) \quad (6)$$

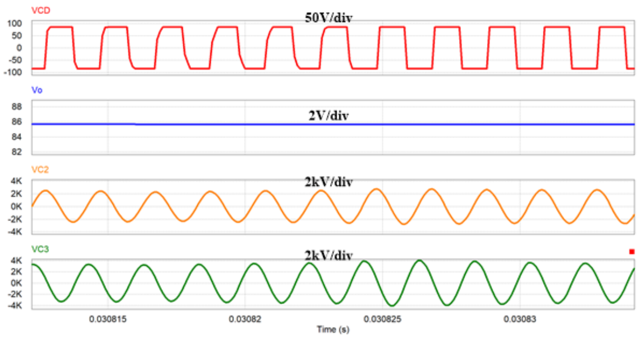


**FIGURE 7.** Operation waveforms of BD-UCWPT system with the load resistance 100Ω in the reverse direction.

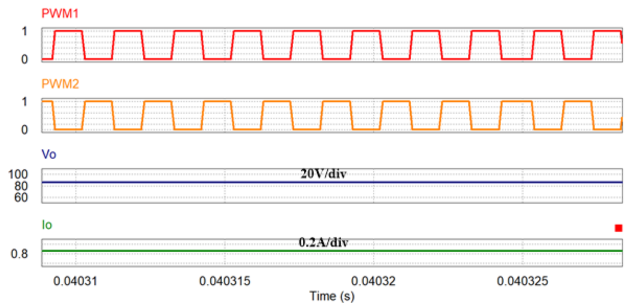


**FIGURE 8.** Simulated load voltage and load current of BD-UCWPT system with the load resistance 100Ω in the reverse direction.

The load voltage and load current are kept stable. The tested load voltage is 78.88V with the input voltage 100V and load resistance 100Ω.

As shown in Fig. 7 and Fig. 8, the BD-UCWPT system works in the reverse direction. The power is wirelessly transferred from $V_L$ to $V_H$. It can be seen from Fig. 7 and Fig. 8, in the the resonnat condition, the tested load voltage is 86.34V with the input voltage 100V and load resistance 100Ω. The load voltage of the proposed BD-UCWPT system is a little higher than that in the forward direction.

The simulated results show that the proposed BD-UCWPT system could transfer the power bidirectionally. As a result, the theory analysis is verified.

The electric field flux of BD-UCWPT system in air and in seawater is shown as Fig. 9. The 3D view of coupling capacitors is shown as Fig. 9(a). It can be seen from Fig. 9(b) and Fig. 9(c), the electric fields distribute in the two channels of two pairs of metal plates. There is leakage electric flux at the edges of metal plates. The electric flux strength of the coupling capacitors in the air as shown in Fig. 9(b) is similar to that in the seawater in Fig. 9(c).

### B. EXPERIMENTAL VERIFICATION

The experiments are conducted to test the performance of proposed BD-UCWPT system. A 100W experimental prototype is shown as Fig. 4. In order to model the seawater condition, two plastic bags with seawater are respectively placed between the four aluminum plates. The aluminum plate is designed with the size 50cm×50cm×0.3cm. In the

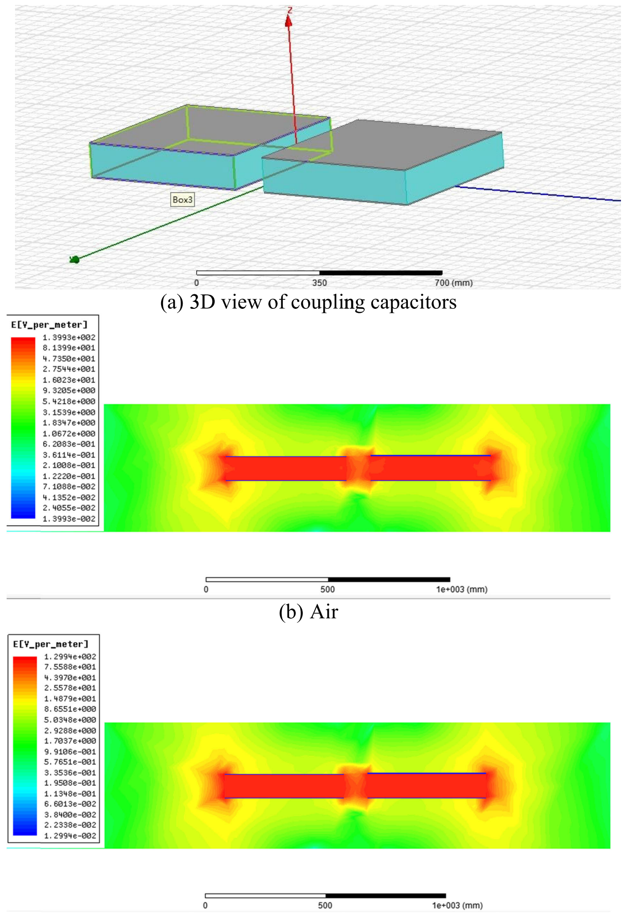


(a) 3D view of coupling capacitors

(b) Air

(c) Seawater

**FIGURE 9.** Simulated electric fields with Ansys Maxwell at the 10cm distance of four metal plates. (a) Three-dimensional of the coupling capacitors, (b) air medium, and (c)seawater medium.

experiments, the range of input voltage is 0-100V.The resonant frequency is 625kHz.

The capacitance of $C_{S1}$ and $C_{S2}$ are tested with air medium and seawater medium, respectively. As shown in Fig. 10, with the air medium the highest capacitance of $C_{S1}$ and $C_{S2}$ is about 100pF at the distance 3cm and the lowest value is about 19pF at the distance 18cm. However, it can be seen from Fig. 11, with the seawater medium, the highest capacitance of $C_{S1}$ and $C_{S2}$ is about 2800pF at the distance 3cm and the lowest value is about 650pF at the distance 18cm. As a result, compared to the air medium, the coupling coefficient and the coupling capacitance is highly improved with the seawater medium. The reason is that the permittivity of seawater is about 81 times bigger than the permittivity of free space. It means that the wireless power transfer could be conducted in the seawater condition with the much longer distance between transmnitter and receiver than in the air condition. It could transfer same power levele with the slower frequency. The tested highest efficiceny is 80.15% at the transfer distance 15cm. The CWPT system provide a very good performacne for the WPT system in seawater condition. It has a bright future to improve the power density in the future work of smart ocean system.

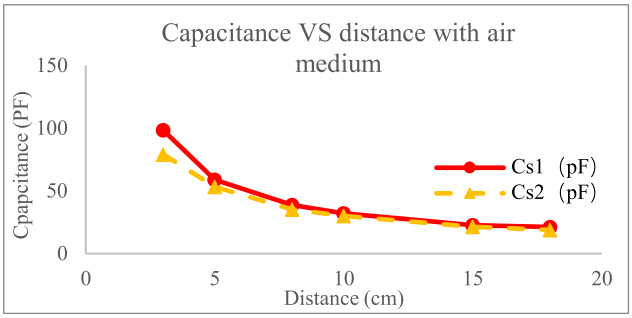


**FIGURE 10.** Coupling capacitance of $C_{S1}$ and $C_{S2}$ with the variable distance with air medium.

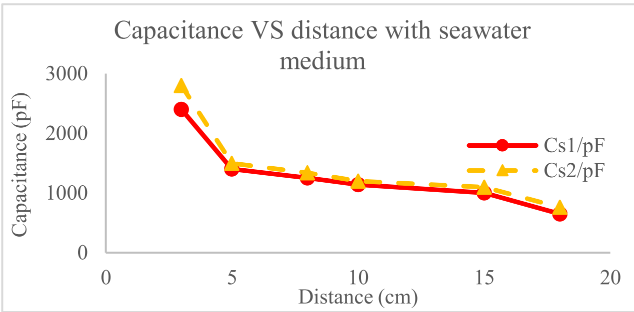


**FIGURE 11.** Coupling capacitance of $C_{S1}$ and $C_{S2}$ with the variable distance with seawater medium.

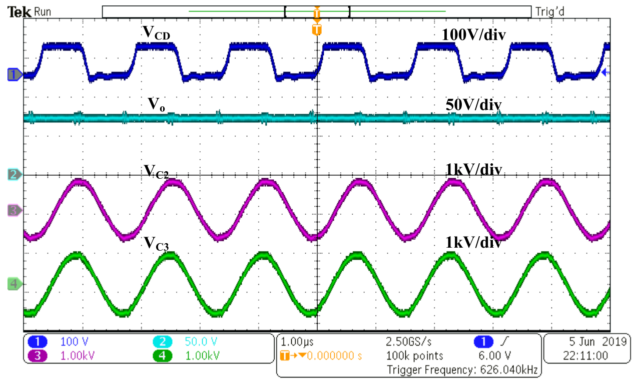


(a) Forward direction

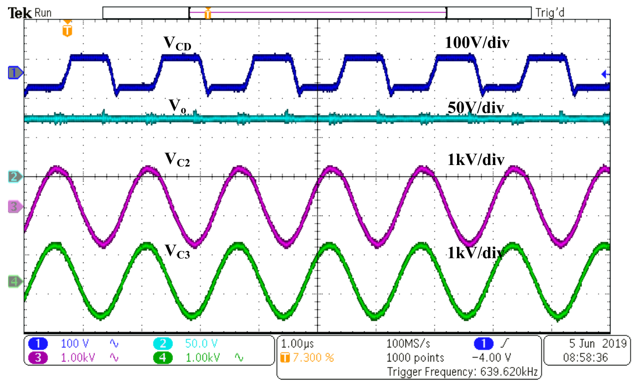


(b) Reverse direction

**FIGURE 12.** Operation waveforms of BD-UCWPT system with Vin = 100V at distance 10 cm between transmitter and receiver (a) forward direction and (b) reverse direction.

In order to verify the theory analysis of the proposed BD-UCWPT system, the experiments are conducted both in the forward power transfer direction and in the reverse power transfer direction. The proposed BD-UCWPT system is controlled by the open-loop synchronous control method. The experimental results are shown as Fig. 12. As shown in Fig. 12(a), in the forward direction, with the seawater medium, the load voltage is kept stable and the value is about 80V. The BD-UCWPT system is in the resonant condition. The voltage of $V_{C2}$ and $V_{C3}$ is sinusoidal wave. The voltage waveform of $V_{C3}$ follows the voltage waveforms of $V_{C2}$. The power of proposed BD-UCWPT system could be robustly transferred with the distance 10cm between transmitter and receiver. It means that the power transfer capacity of the proposed BD-UCWPT system is good. Experimental results agree well with the simulation and theory analysis.

As shown in Fig. 12(b), in the reverse direction, the voltage waveform of $V_{C2}$ follows the voltage waveforms of $V_{C3}$, the load voltage is also kept stable in the reverse condition. As shown in Fig. 12 (b), with the load resistance 100Ω, the load voltage is about 80V at the distance 10cm between transmitter and receiver.

It can be seen from the experimental results as shown in Fig. 12, with the seawater medium, the power could be bidirectionally transferred between transmitter and receiver under resonant condition. With the open-loop synchronous control method, the load power could be maintained stable. At the same tested condition, the load power in the forward direction is similar to the power level in the reverse direction. The experimental results match very well with the simulated results.

### C. COMPARISON WITH OTHER UWPT SYSTEMS

The comparison with other UWPT systems in terms of power level, operating frequency, efficiency, transfer distance and so on is shown in Table 1. It can be seen from Table 1, with the proposed UWPT system in this paper, the power could be transferred bidirectionally with over 80% efficiency for seawater at large distance. The capacitive UWPT system could be conducted by a simple structure consisting of four meatal plates. Compared with the inductive UWPT systems as shown in [19], [21] and [37]–[40], the power for capacitive UWPT is transferred by electric fields concentrated between the electrodes, the amount of the current on the electrodes of the coupler is very low, and the generation of heat due to ohmic loss is reduced. The eddy current losses which is generated by the magnetic fields in the metals located near the inductive UWPT system could be also removed with the proposed UWPT system. It is not sensitive to conductive objects.

## IV. CONCLUSIONS AND DISCISSONS

This paper proposes a BD-UCWPT system for the AUVs. With the proposed BD-UCWPT system, the AUVs could be charged by the undersea wireless charge station and discharge its energy to other AUV or undersea sensors. In this paper, the CWPT system is firstly adapted in the undersea condition. A 100W experimental BD-UCWPT system is built. The two pairs of metal plates are acted as the WPT unit. The power is wirelessly transferred through the electric fields. The resonant frequency is set 625KHz. The theory analysis and functions of proposed BD-UCWPT system are verified with the simulation and experiments. The experimental results show that the power could be transferred bidirectionally between $V_H$ side and $V_L$ side. It has been done with air medium and seawater medium. The proposed BD-UCWPT system could work well in seawater. The GaN based H-Bridge could help reduce switching power loss in high switching frequency. With this BD-UCWPT system, AUVs could be conveniently charged in the undersea condition. This WPT system will facilitate the AUVs application and improve the smart ocean energy development in the future with an alternative undersea wireless charging method.

## REFERENCES

[1] B. Minnaert and N. Stevens, "Design of a capacitive wireless power transfer link with minimal receiver circuitry," in *Proc. IEEE PELS Workshop Emerg. Technol., Wireless Power Transf. (Wow)*, Montréal, QC, Canada, Jun. 2018, pp. 1–5.

[2] C.-H. Jeong, P.-H. La, S.-J. Choi, and H.-S. Choi, "A novel target detection algorithm for capacitive power transfer systems," in *Proc. IEEE Appl. Power Electron. Conf. Expo. (APEC)*, San Antonio, TX, USA, Mar. 2018, pp. 3174–3177.

[3] E. Abramov, I. Zeltser, and M. M. Peretz, "A network-based approach for modeling resonant capacitive wireless power transfer systems," *CPSS Trans. Power Electron. Appl.*, vol. 4, no. 1, pp. 19–29, Mar. 2019.

[4] D. C. Corrêa, U. C. Resende, and F. S. Bicalho, "Experiments with a compact wireless power transfer system using strongly coupled magnetic resonance and metamaterials," *IEEE Trans. Magn.*, vol. 55, no. 8, Aug. 2019, Art. no. 8401904. doi: 10.1109/TMAG.2019.2913767.

[5] Y. Li, J. Hu, X. Li, and K.-W. E. Cheng, "A flexible load-independent multi-output wireless power transfer system based on cascaded double T-resonant circuits: Analysis, design and experimental verification," *IEEE Trans. Circuits Syst. I, Reg. Papers*, vol. 66, no. 7, pp. 2803–2812, Jul. 2019. doi: 10.1109/TCSI.2019.2899431.

[6] C. Cheng, F. Lu, Z. Zhou, W. Li, C. Zhu, H. Zhang, Z. Deng, X. Chen, and C. C. Mi, "Load-independent wireless power transfer system for multiple loads over a long distance," *IEEE Trans. Power Electron.*, vol. 34, no. 9, pp. 9279–9288, Sep. 2019. doi: 10.1109/TPEL.2018.2886329.

[7] J. P.-W. Chow, H. S.-H. Chung, L. L.-H. Chan, R. Shen, and S. C. Tang, "Optimal design and experimental assessment of a wireless power transfer system for home-cage monitoring," *IEEE Trans. Power Electron.*, vol. 34, no. 10, pp. 9779–9793, Oct. 2019. doi: 10.1109/TPEL.2019.2894182.

[8] K. Hassan, S. Pan, and P. Jain, "Multiple receiver wireless power charger for mobile electronic devices in near field," in *Proc. IEEE Int. Conf. Ind. Electron. Sustain. Energy Syst. (IESES)*, Hamilton, New Zealand, Jan./Feb. 2018, pp. 426–433.

[9] M. Huang, Y. Lu, and R. P. Martins, "A reconfigurable bidirectional wireless power transceiver for battery-to-battery wireless charging," *IEEE Trans. Power Electron.*, vol. 34, no. 8, pp. 7745–7753, Aug. 2019. doi: 10.1109/TPEL.2018.2881285.

[10] N. Ha-Van and C. Seo, "Butterfly-shaped transmitting coil for wireless power transfer system in millimeter-sized biomedical implants," in *Proc. IEEE Wireless Power Transf. Conf. (WPTC)*, Montreal, QC, Canada, Jun. 2018, pp. 1–4.

[11] Z. Wang and S. Mirabbasi, "A low-voltage CMOS rectifier with on-chip matching network and a magnetic field focused antenna for Wirelessly powered medical implants," *IEEE Trans. Biomed. Circuits Syst.*, vol. 13, no. 3, pp. 554–565, Jun. 2019. doi: 10.1109/TBCAS.2019.2904487.

[12] T. Li, Z. Han, H. Ogai, K. Sawada, and J. Wang, "A microchip-controlling wireless power transfer system for sensor network," in *Proc. SICE Annu. Conf. (SICE)*, Akita, Japan, Aug. 2012, pp. 337–341.

[13] Z. Wang, L. Duan, and R. Zhang, "Adaptively directional wireless power transfer for large-scale sensor networks," *IEEE J. Sel. Areas Commun.*, vol. 34, no. 5, pp. 1785–1800, May 2016.

[14] O. C. Onar, M. Chinthavali, S. L. Campbell, L. E. Seiber, C. P. White, and V. P. Galigekere, "Modeling, simulation, and experimental verification of a 20-kW series-series wireless power transfer system for a toyota RAV4 electric vehicle," in *Proc. IEEE Transp. Electrific. Conf. Expo (ITEC)*, Long Beach, CA, USA, Jun. 2018, pp. 874–880.

[15] B. Regensburger, J. Estrada, A. Kumar, S. Sinha, Z. Popović, and K. K. Afridi, "High-performance capacitive wireless power transfer system for electric vehicle charging with enhanced coupling plate design," in *Proc. IEEE Energy Convers. Congr. Expo. (ECCE)*, Portland, OR, USA, Sep. 2018, pp. 2472–2477.

[16] H. Li, J. Fang, and Y. Tang, "Dynamic phasor-based reduced order models of wireless power transfer systems," *IEEE Trans. Power Electron.*, to be published. doi: 10.1109/TPEL.2019.2897823.

[17] C. Cai, M. Qin, S. Wu, and Z. Yang, "A strong misalignmentt tolerance magnetic coupler for autonomous underwater vehicle wireless power transfer system," in *Proc. IEEE Int. Power Electron. Appl. Conf. Expo. (PEAC)*, Shenzhen, China, Nov. 2018, pp. 1–5.

[18] Z. Yan, B. Song, Y. Zhang, K. Zhang, Z. Mao, and Y. Hu, "A rotation-free wireless power transfer system with stable output power and efficiency for autonomous underwater vehicles," *IEEE Trans. Power Electron.*, vol. 34, no. 5, pp. 4005–4008, May 2019.

[19] T. Kan, R. Mai, P. P. Mercier, and C. C. Mi, "Design and analysis of a three-phase wireless charging system for lightweight autonomous underwater vehicles," *IEEE Trans. Power Electron.*, vol. 33, no. 8, pp. 6622–6632, Aug. 2018.

[20] Z. Yan, Y. Zhang, T. Kan, F. Lu, K. Zhang, B. Song, and C. C. Mi, "Frequency optimization of a loosely coupled underwater wireless power transfer system considering eddy current loss," *IEEE Trans. Ind. Electron.*, vol. 66, no. 5, pp. 3468–3476, May 2019.

[21] T. Orekan, P. Zhang, and C. Shih, "Analysis, design, and maximum power-efficiency tracking for undersea wireless power transfer," *IEEE J. Emerg. Sel. Topics Power Electron.*, vol. 6, no. 2, pp. 843–854, Jun. 2018.

[22] D. Futagami, Y. Sawahara, T. Ishizaki, and I. Awai, "Study on high efficiency WPT underseas," in *Proc. IEEE Wireless Power Transf. Conf. (WPTC)*, Boulder, CO, USA, May 2015, pp. 1–4.

[23] F. Lu, H. Zhang, H. Hofmann, and C. Mi, "A double-sided LCLC-compensated capacitive power transfer system for electric vehicle charging," *IEEE Trans. Power Electron.*, vol. 30, no. 11, pp. 6011–6014, Nov. 2015.

[24] H. Zhang, F. Lu, H. Hofmann, W. Liu, and C. C. Mi, "A four-plate compact capacitive coupler design andLCL-compensated topology for capacitive power transfer in electric vehicle charging application," *IEEE Trans. Power Electron.*, vol. 31, no. 12, pp. 8541–8551, Dec. 2016.

[25] X. Li, C. Tang, X. Dai, P. Deng, and Y. Su, "An inductive and capacitive combined parallel transmission of power and data for wireless power transfer systems," *IEEE Trans. Power Electron.*, vol. 33, no. 6, pp. 4980–4991, Jun. 2018.

[26] T. M. Mostafa, A. Muharam, and R. Hattori, "Wireless battery charging system for drones via capacitive power transfer," in *Proc. IEEE PELS Workshop Emerg. Technol., Wireless Power Transf. (WoW)*, Chongqing, China, May 2017, pp. 1–6.

[27] N. Sakai, D. Itokazu, Y. Suzuki, S. Sakihara, and T. Ohira, "One-kilowatt capacitive Power Transfer via wheels of a compact electric vehicle," in *Proc. IEEE Wireless Power Transf. Conf. (WPTC)*, Aveiro, Portugal, May 2016, pp. 1–3.

[28] B. Minnaert and N. Stevens, "Power maximization for capacitive wireless power transfer with two transmitters and one receiver," in *IEEE MTT-S Int. Microw. Symp. Dig.*, Chengdu, China, May 2018, pp. 1–4.

[29] D. Shmilovitz, A. Abramovitz, and I. Reichman, "Quasi-resonant LED driver with capacitive isolation and high PF," *IEEE J. Emerg. Sel. Topics Power Electron.*, vol. 3, no. 3, pp. 633–641, Sep. 2015.

[30] L. Huang, A. P. Hu, A. K. Swain, and Y. G. Su, "Z-impedance compensation for wireless power transfer based on electric field," *IEEE Trans. Power Electron.*, vol. 31, no. 11, pp. 7556–7563, Nov. 2016.

[31] A. Muharam, T. M. Mostafa, A. Nugroho, and R. Hattori, "Power loss analysis of inverter with and without transformer for capacitive power transfer," in *Proc. IEEE Wireless Power Transf. Conf. (WPTC)*, Montreal, QC, Canada, Jun. 2018, pp. 1–4.

[32] T. M. Mostafa, D. Bui, A. Muharam, R. Hattori, and A. P. Hu, "A capacitive power transfer system with a CL network for improved system performance," in *Proc. IEEE Wireless Power Transf. Conf. (WPTC)*, Montreal, QC, Canada, Jun. 2018, pp. 1–4.

[33] S. Sinha, B. Regensburger, A. Kumar, and K. Afridi, "A very-high-power-transfer-density GaN-based capacitive wireless power transfer system," in *Proc. IEEE 5th Workshop Wide Bandgap Power Devices Appl. (WiPDA)*, Albuquerque, NM, USA, Oct./Nov. 2017, pp. 360–365.

[34] D. Bui, T. M. Mostafa, A. P. Hu, and R. Hattori, "DC-DC converter based impedance matching for maximum power transfer of CPT system with high efficiency," in *Proc. IEEE PELS Workshop Emerg. Technol., Wireless Power Transf. (Wow)*, Montréal, QC, Canada, Jun. 2018, pp. 1–5.

[35] M. Tamura, Y. Naka, K. Murai, and T. Nakata, "Design of a capacitive wireless power transfer system for operation in fresh water," *IEEE Trans. Microw. Theory Techn.*, vol. 66, no. 12, pp. 5873–5884, Dec. 2018.

[36] L. Klein and C. T. Swift, "An improved model for the dielectric constant of sea water at microwave frequencies," *IEEE Trans. Antennas Propag.*, vol. AP-25, no. 1, pp. 104–111, Jan. 1977.

[37] Y. Sawahara, D. Futagami, T. Ishizaki, and I. Awai, "Development of underwater WPT system independent of salinity," in *Proc. Asia–Pacific Microw. Conf.*, Sendai, Japan, Nov. 2014, pp. 1363–1365.

[38] A. Askari, R. Stark, J. Curran, D. Rule, and K. Lin, "Underwater wireless power transfer," in *Proc. IEEE Wireless Power Transf. Conf.*, Boulder, CO, USA, May 2015, pp. 1–4.

[39] M. Ogihara, T. Ebihara, K. Mizutani, and N. Wakatsuki, "Wireless power and data transfer system for station-based autonomous underwater vehicles," in *Proc. MTS/IEEE OCEANS*, Washington, DC, USA, Oct. 2015, pp. 1–5.

[40] V. Bana, M. Kerber, G. Anderson, J. D. Rockway, and A. Phipps, "Undersea wireless power transfer for maritime applications," in *Proc. IEEE Wireless Power Transf. Conf. (WPTC)*, Boulder, CO, USA, 2015, pp. 1–4.

**LEI YANG** (S'15–M'17) was born in Henan, China, in 1986. He received the B.S. degree in electric and information engineering from Information Engineering University, Zhengzhou, China, in 2011, and the M.S. degree in signal and information processing (SIP) and the Ph.D. degree in electrical engineering from Northwestern Polytechnical University, Xi'an, China, in April 2014 and in June 2017, respectively.

From September 2014 to September 2016, he was a Visiting Student with the University of California at Irvine, Irvine, CA, USA. He is currently an Assistant Professor with the Xi'an University of Technology. His interests include nonlinear control, switched-capacitor (SC) converters, DC–DC converters, the power source of electrical vehicles, wireless power and data transfer systems, and renewable energy integration.

**MINNA JU** was born in Shaanxi, China, in 1998. She received the B.S. degree in electrical engineering and automation from the Xi'an University of Technology, Xi'an, Shaanxi, in June 2019. She is currently working as an R&D Assistant Engineer with Zhuhai Enpower Electric Company Ltd. Her research interests include wireless charging, DC–DC converters, and bidirectional OBC technology.

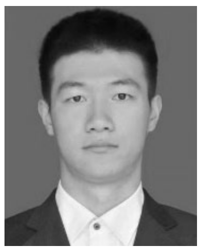

**BEN ZHANG** was born in Shaanxi, China, in 1997. He received the B.S. degree in electrical engineering and automation from the Xi'an University of Technology, Xi'an, Shaanxi, China, in June 2019, where he is currently a member of the Research and Development Team, Shaanxi Automobile Holding Group. His main research direction includes the control strategy of wireless power transmission systems and bidirectional DC–DC converters.